

Figures and captions

Fig. 1. Molecular structure of C₂₅ highly branched isoprenoid (HBI) alkenes and sterols described in the text. IP₂₅ (C_{25:1}), HBI-II (C_{25:2}), HBI-III (C_{25:3}), brassicasterol and dinosterol. Carbon labeling is shown on the structure of IP₂₅.

Fig. 2. Map of the surface ocean circulation in the study area (after Danielson et al., 2011) and sampling locations. The red dot indicates the mooring site (station DM) and black dots indicate the locations where the surface sediments were sampled. The yellow dots in the upper left insert show the locations of all sediment trap sites discussed in the text (Fahl and Nöthig, 2007; Lalande et al., 2009; Watanabe et al., 2014),.

Fig. 3. Time series of bulk parameters measured at station DM from August 2008 to September 2009. (a) Temporal evolution of sea ice concentration (in %; from Cavalieri et al., 1996). (b) C:N ratio (blue line) and particulate organic carbon (% POC; orange line). (c) Total mass flux (mg m⁻²d⁻¹). (d) POC flux (mg m⁻²d⁻¹). The blue shaded area shows the period of sea ice coverage.

Fig. 4. Time series of sea ice concentration, and Σ ALK₂₇₋₃₁, brassicasterol and dinosterol fluxes at station DM from August 2008 to September 2009. (a) Temporal evolution of sea ice concentration (in %; from Cavalieri et al., 1996). (b) Daily flux of the odd-carbon-numbered n-alkanes from C₂₇ to C₃₁ (Σ ALK₂₇₋₃₁; μ g m⁻²d⁻¹). (c) Daily flux of brassicasterol (μ g m⁻²d⁻¹). (d) Daily flux of dinosterol (μ g m⁻²d⁻¹). The blue shaded area shows the period of sea ice coverage.

Fig. 5. Time series of sea ice concentration, fluxes of IP₂₅, HBI-II, HBI-III, brassicasterol and PIP₂₅ indexes at station DM from August 2008 to September 2009. (a) Temporal evolution of sea ice concentration (in %; from Cavalieri et al., 1996). (b) Flux of IP₂₅ (ng m⁻²d⁻¹ relative to the internal standard). (c) Flux of HBI-II (ng m⁻²d⁻¹ relative to the internal standard). (d) Flux of HBI-III (ng m⁻²d⁻¹ relative to

the internal standard). (e) Flux of brassicasterol ($\mu\text{g m}^{-2}\text{d}^{-1}$). (f) PIP_{25} index based on brassicasterol ($\text{P}_{\text{B}}\text{IP}_{25}$, $c = 0.00393$). (g) PIP_{25} index based on HBI-III ($\text{P}_{\text{III}}\text{IP}_{25}$, for $c = 10.943$ and $c = 1$). The blue shaded area shows the period of sea ice coverage.

Fig. 6. Spatial distribution of sea ice concentrations and biomarkers in the western Arctic Ocean. (a) Spring (April–June) sea ice concentration from 1988 to 2007 from <http://www.nsidc.org>. (b) Summer (July–September) sea ice concentration from 1988 to 2007 from <http://www.nsidc.org>. (c) Concentrations of the open-water phytoplankton biomarker brassicasterol ($\mu\text{g/g OC}$). (d) Concentrations of the open-water phytoplankton biomarker dinosterol ($\mu\text{g/g OC}$). (e) IP_{25} ($\mu\text{g/g OC}$ relative to the internal standard). (f) HBI-II ($\mu\text{g/g OC}$ relative to the internal standard). (g) HBI-III ($\mu\text{g/g OC}$ relative to the internal standard). Black dots indicate the locations of the surface sediment sites. The dash-dotted and dashed lines represent the 15% and 80% isolines, respectively, of summer sea ice cover for the period 1988–2007.

Fig. 7. Spatial distribution of the PIP_{25} index and correlations against spring/summer sea ice concentrations derived from satellite data. (a) The $\text{P}_{\text{B}}\text{IP}_{25}$ index ($c = 0.1063$). (b) The $\text{P}_{\text{III}}\text{IP}_{25}$ index ($c = 3.7111$). (c) Correlation between $\text{P}_{\text{B}}\text{IP}_{25}$ ($c = 0.1063$) and spring sea ice concentration. (d) Correlation between $\text{P}_{\text{III}}\text{IP}_{25}$ ($c = 3.7111$) and spring sea ice concentration. (e) Correlation between $\text{P}_{\text{B}}\text{IP}_{25}$ ($c = 0.1063$) and summer sea ice concentration. (f) Correlation between $\text{P}_{\text{III}}\text{IP}_{25}$ ($c = 3.7111$) and summer sea ice concentration. Black dots indicate surface sediment samples. The dash-dotted and dashed lines represent the 15% and 80% isolines, respectively, of summer sea ice cover for the period 1988–2007.

Fig. 8. Crossplots of biomarker concentrations. (a) IP_{25} against HBI-II. (b) IP_{25} against HBI-III. (c) HBI-II against HBI-III. Concentrations are expressed as abundances relative to the internal standard and normalized to organic carbon ($\mu\text{g/g OC}$).

Fig. 9. Spatial representations of the PIP_{25} index calculated using different phytoplankton markers and c factors, and correlations between spring/summer sea ice concentrations (derived from satellite data) and PIP_{25} . (a) The P_BIP_{25} index ($c = 0.023$; i.e., the global c factor of Xiao et al. (2015)). (b) The $P_{III}IP_{25}$ index ($c = 1$). (c) Correlation between P_BIP_{25} ($c = 0.023$) and spring sea ice concentration. (d) Correlation between $P_{III}IP_{25}$ ($c = 1$) and spring sea ice concentration. (e) Correlation between P_BIP_{25} ($c = 0.023$) and summer sea ice concentration. (f) Correlation between $P_{III}IP_{25}$ ($c = 1$) and summer sea ice concentration. Black dots indicate surface sediment samples. The dash-dotted and dashed lines represent the 15% and 80% isolines, respectively, of summer sea ice cover for the period 1988–2007.

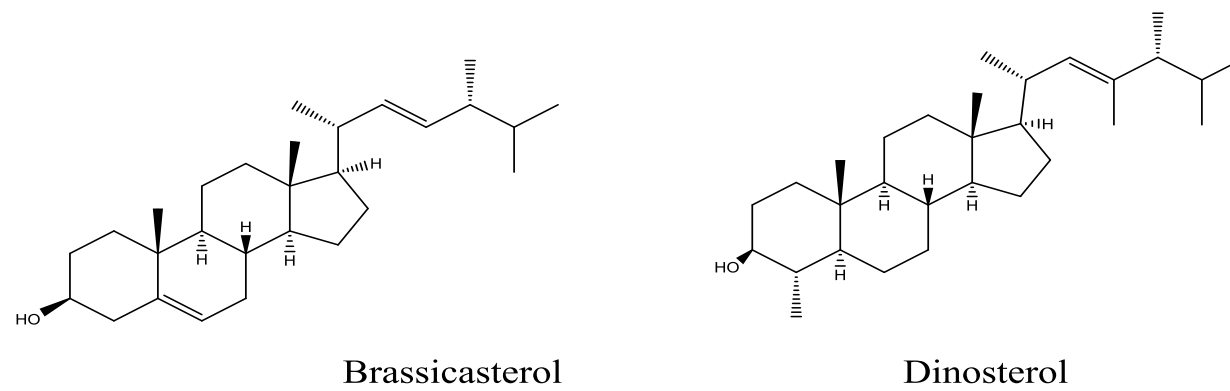
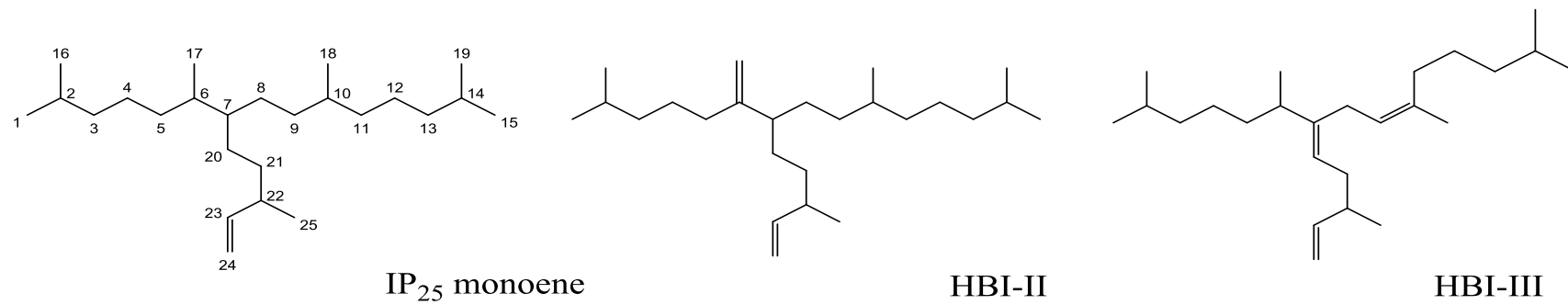


Figure 1.

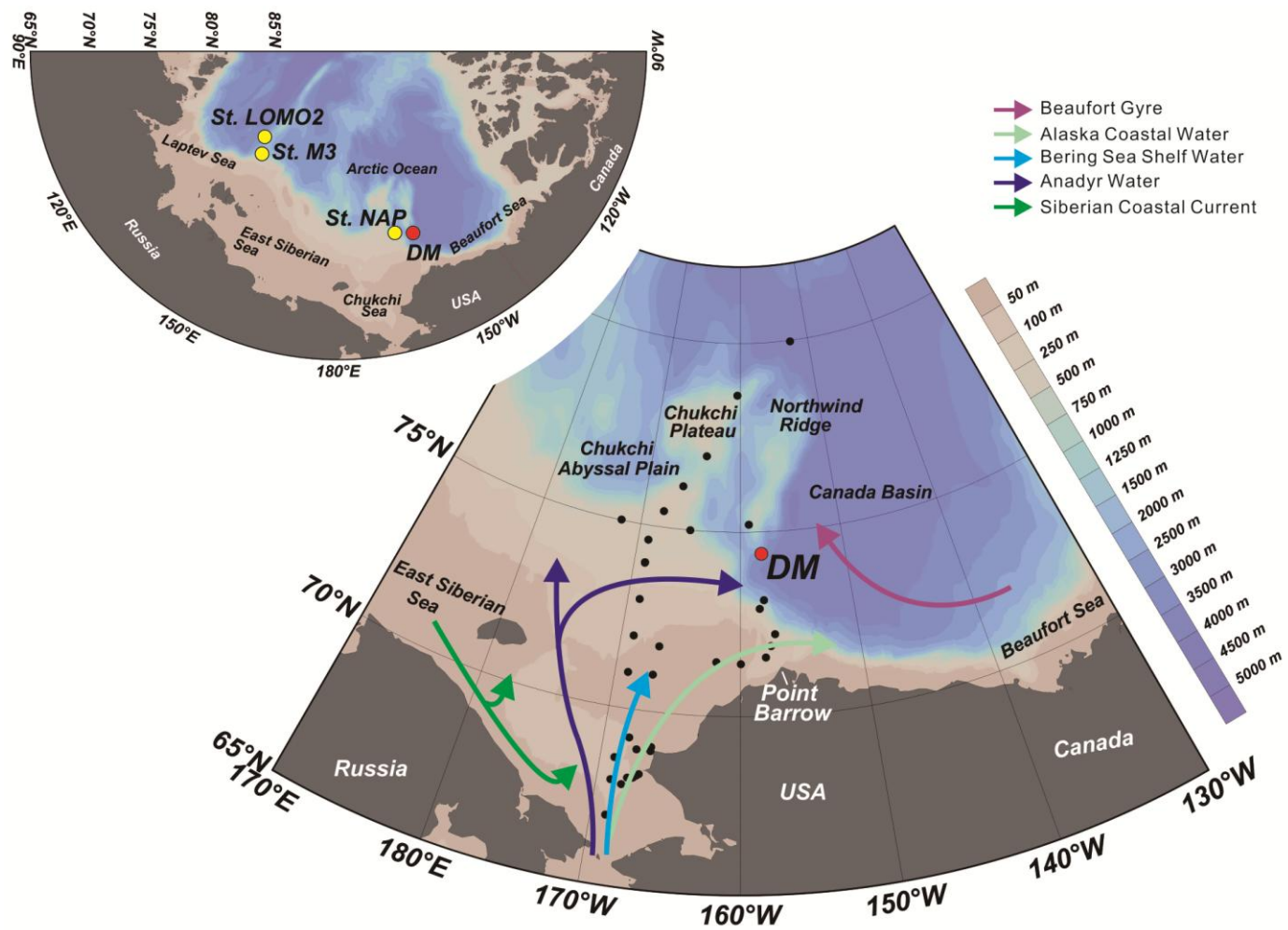


Figure 2.

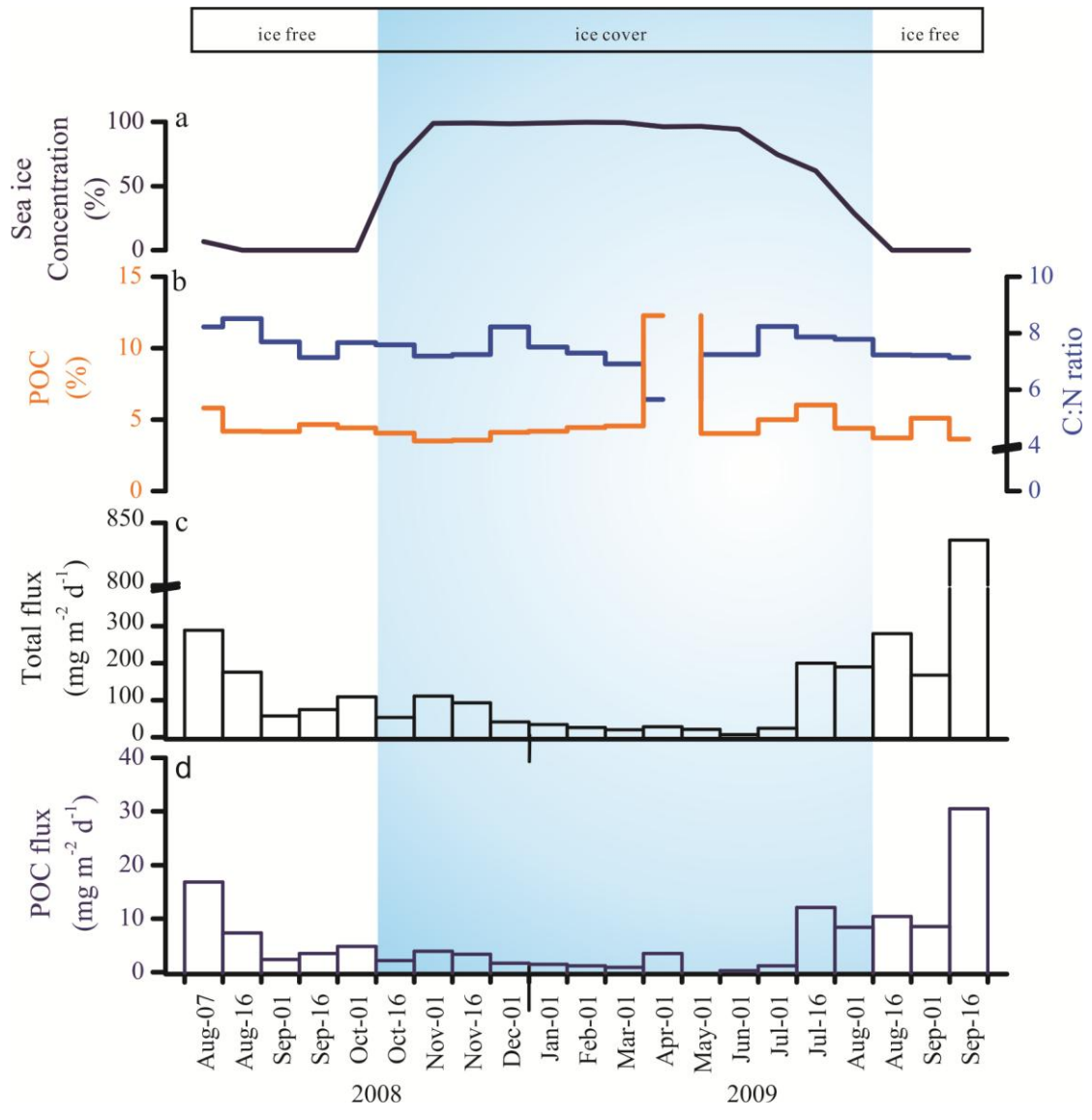


Figure 3.

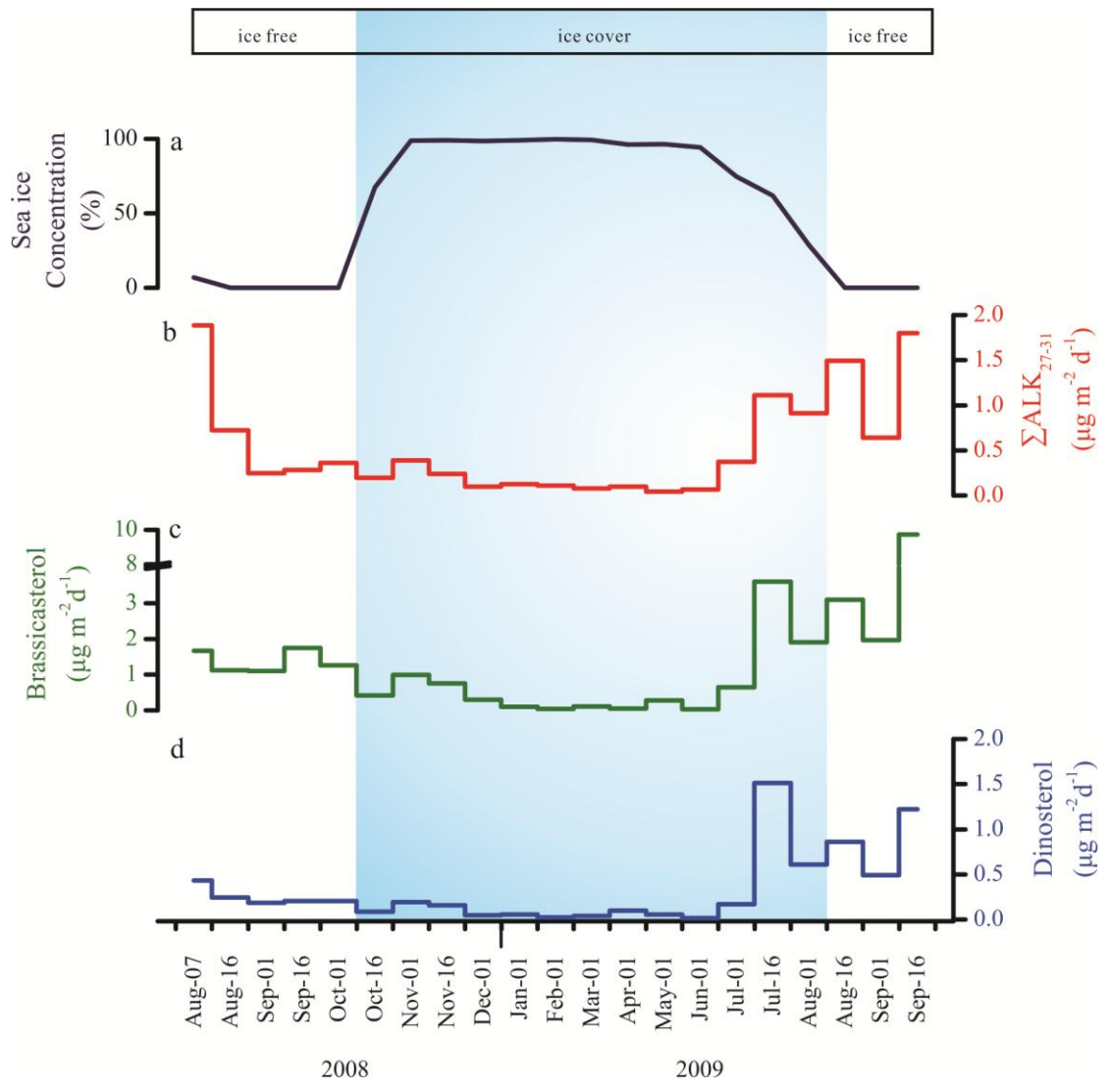


Figure 4.

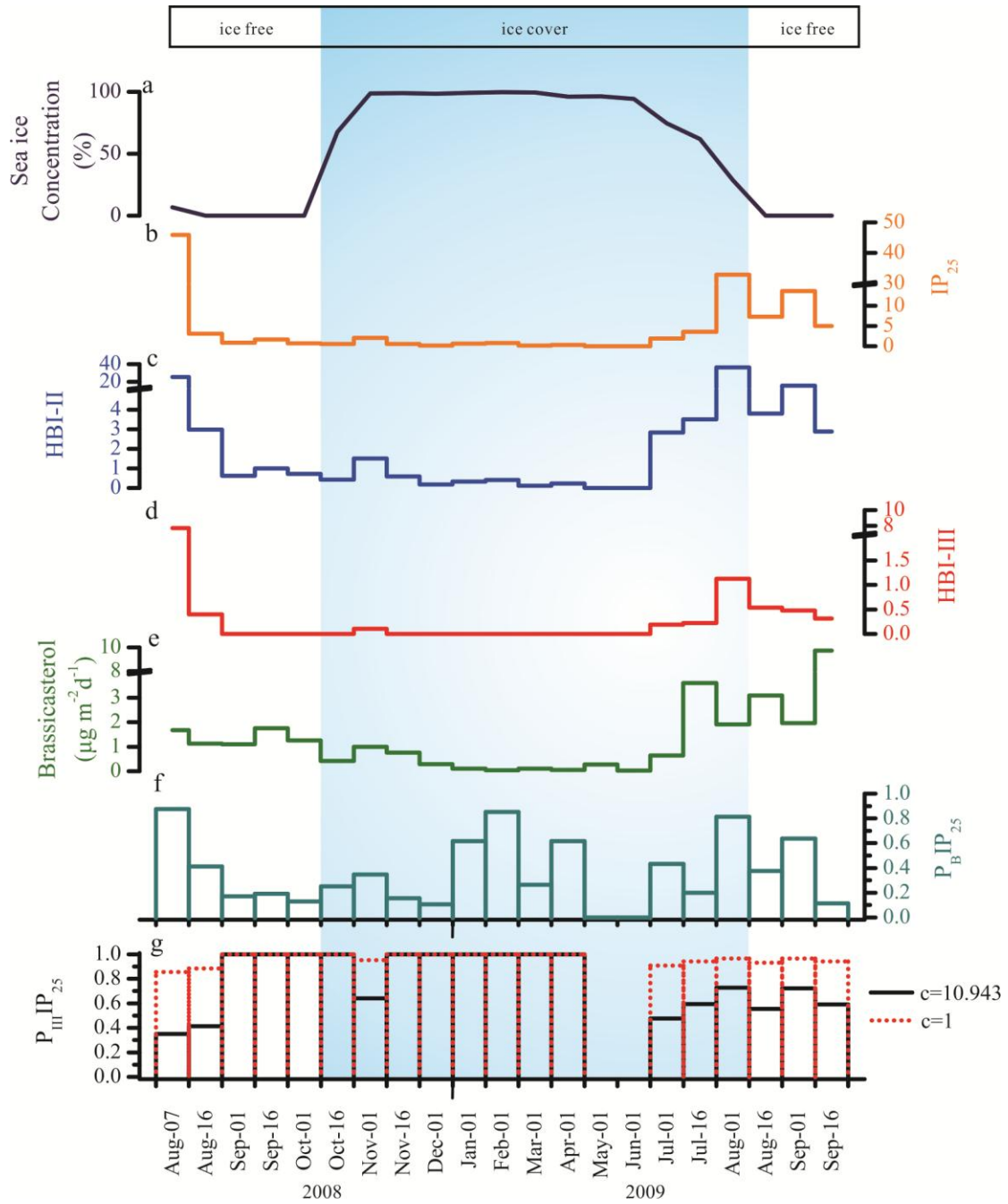


Figure 5.

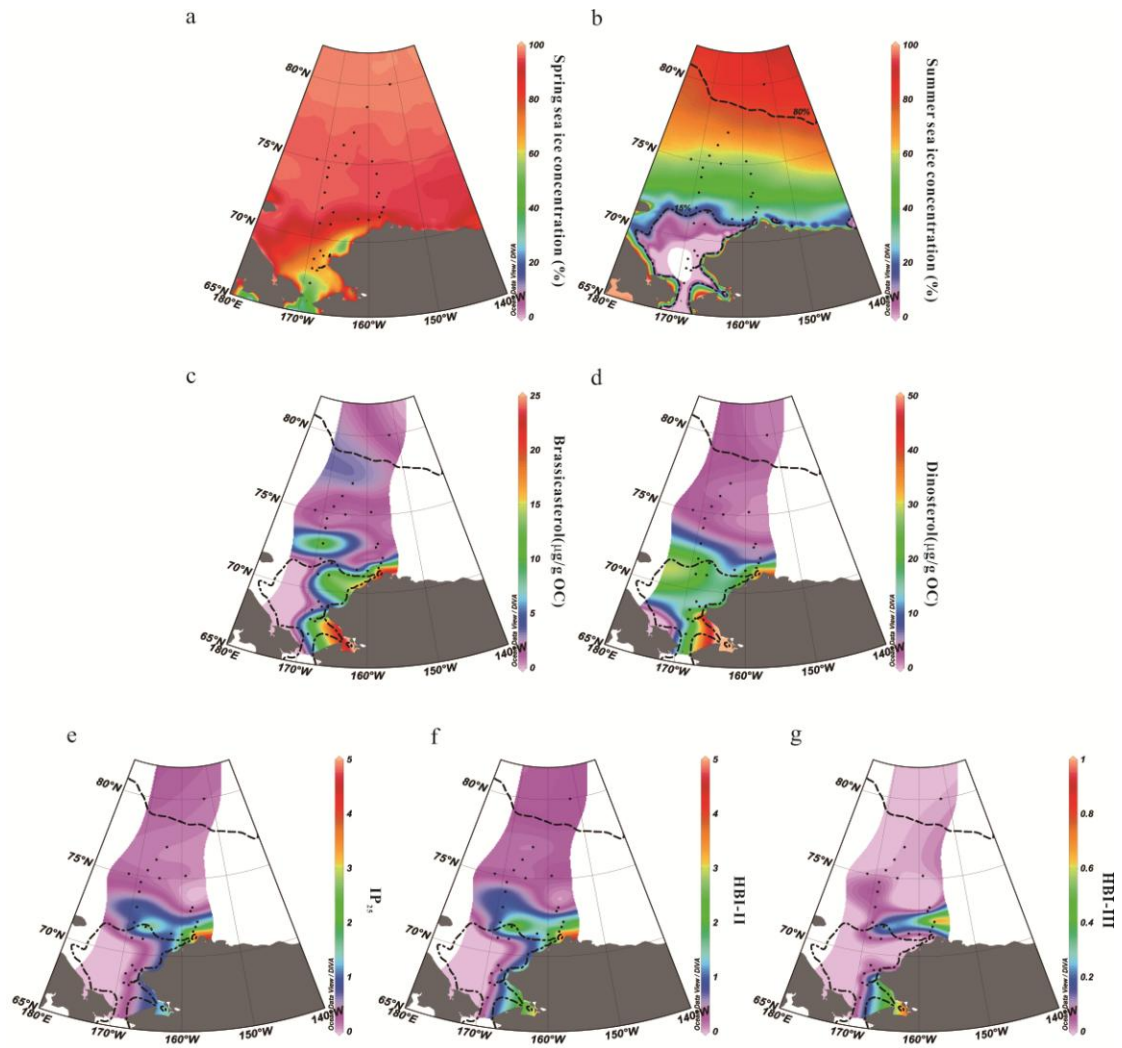


Figure 6.

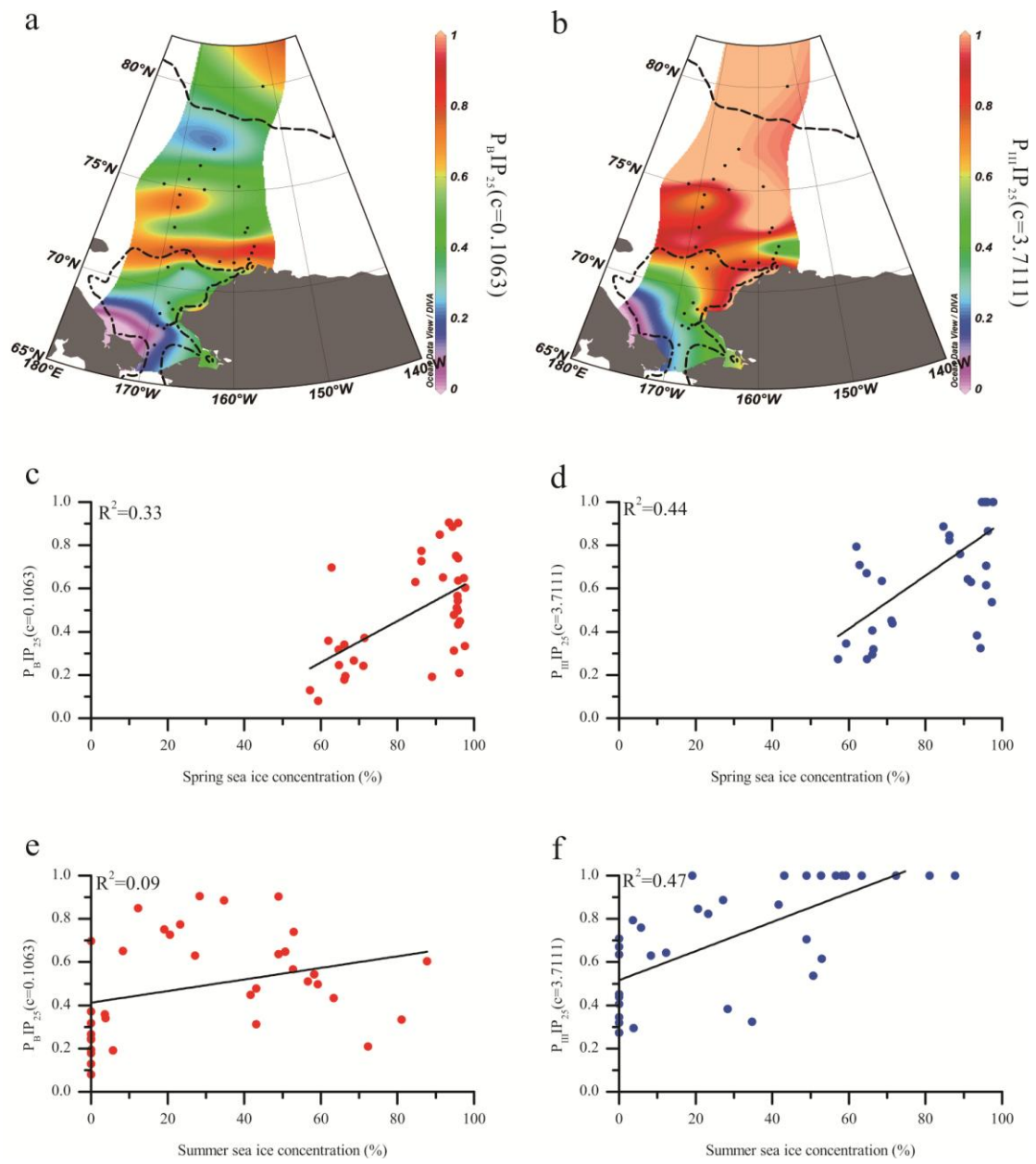


Figure 7.

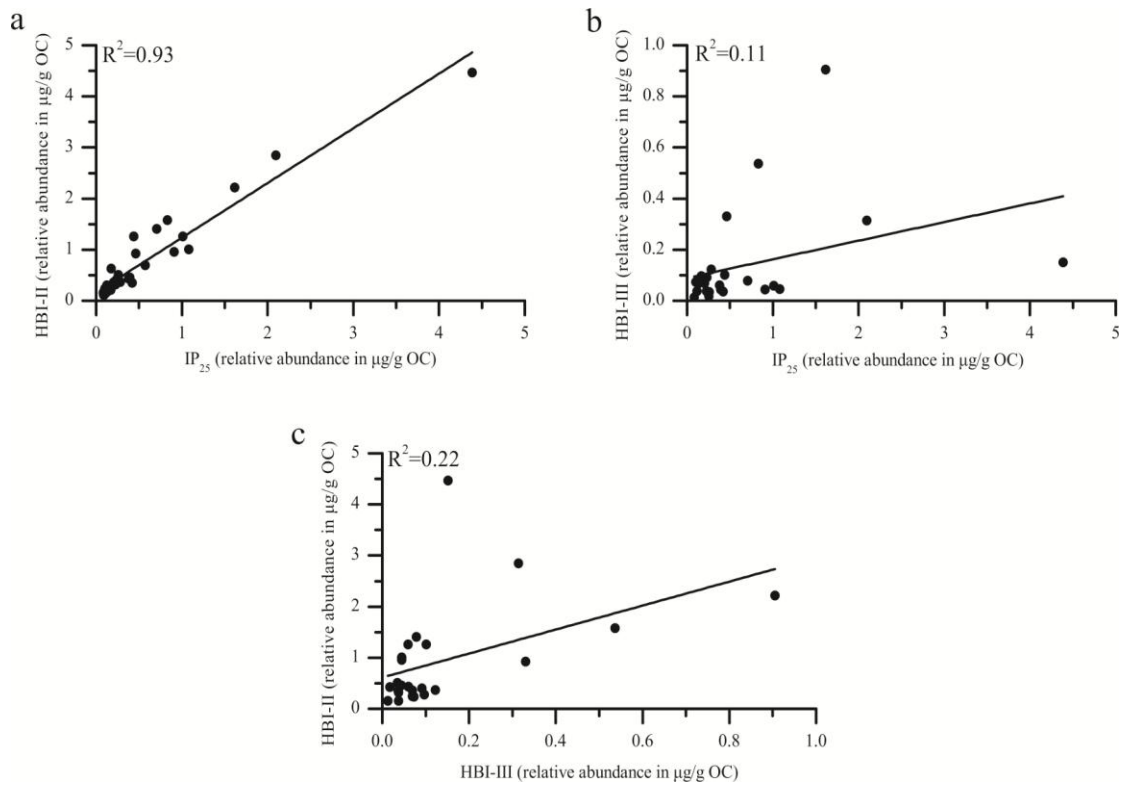


Figure 8.

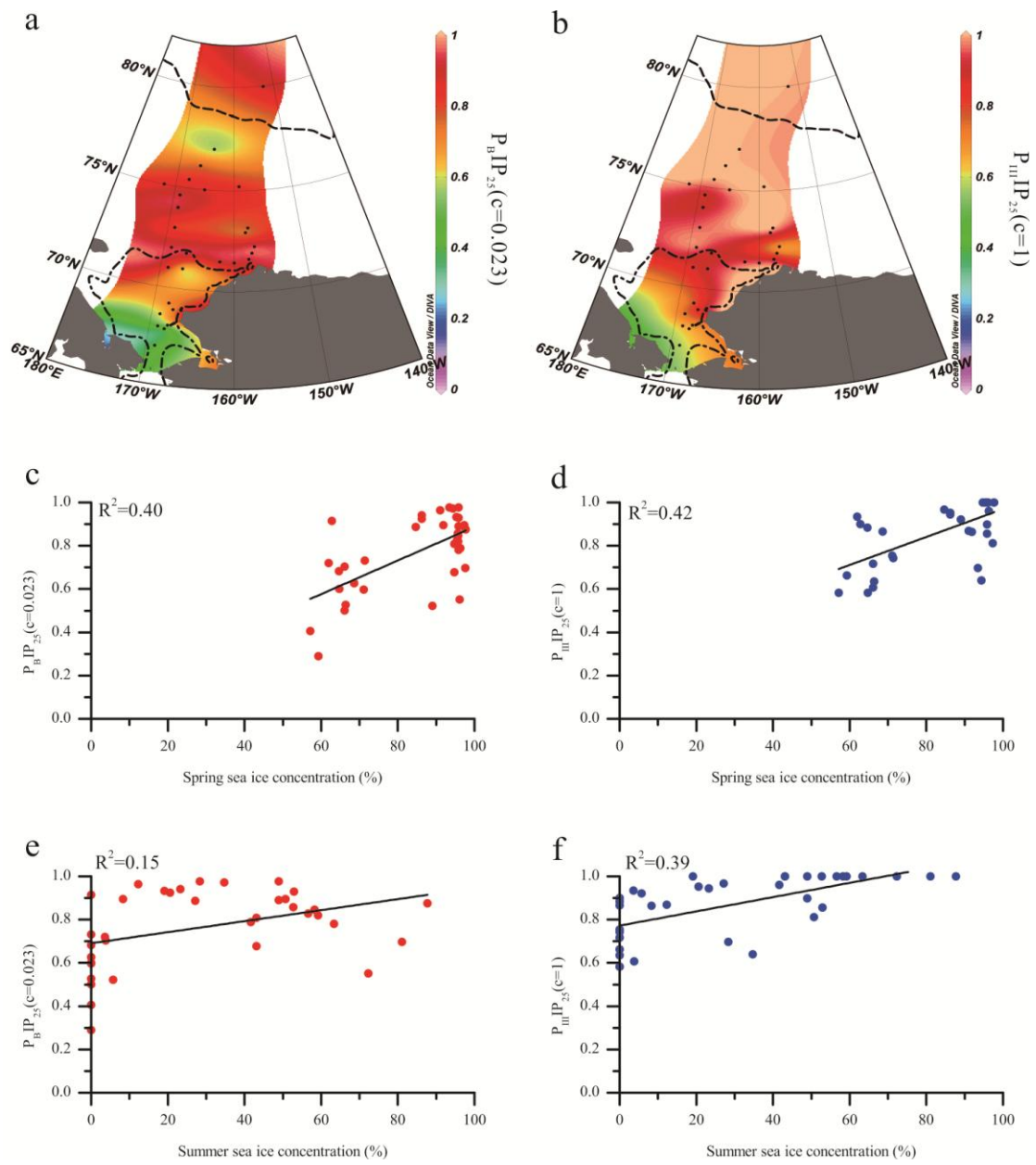


Figure 9.